ORIGINAL RESEARCH

Moderate-Intensity Ultrasound-Triggered On-Demand Analgesia Nanoplatforms for Postoperative Pain Management

Xinye Song[1],*, Mengxiao Luan [ID][2],*, Weiyi Zhang [ID][1], Ruizheng Zhang [ID][1], Li Xue [ID][1], Yong Luan[1]

[1]Department of Anesthesiology, the First Affiliated Hospital of Dalian Medical University, Dalian, 116011, People's Republic of China; [2]Department of Biomedical Engineering, Tsinghua University, Beijing, 100084, People's Republic of China

*These authors contributed equally to this work

Correspondence: Yong Luan, Email luanyong@dmu.edu.cn

Introduction: The restricted duration is a fundamental drawback of traditional local anesthetics during postoperative pain from a single injection. Therefore, an injectable local anesthetic that produces repeatable on-demand nerve blocks would be ideal.

Methods: We offer ultrasound-triggered on-demand analgesia consisting of dendritic mesoporous silica nanoparticles (DMSN) carried with ultrasound-sensitive perfluoropentane (PFP) and levobupivacaine (DMSN-bupi-PFP) to achieve repeatable and customizable on-demand local anesthetics.

Results: The vaporization of liquid PFP was triggered by ultrasound irradiation to produce a gas environment. Subsequently, the enhanced cavitation effect could improve the release of levobupivacaine to achieve pain relief under a moderate-intensity ultrasound irradiation. DMSN-bupi-PFP demonstrated a controlled-release pattern and showed a reinforced ultrasonic sensitivity compared to levobupivacaine loaded DMSN (DMSN-bupi). The sustained release of levobupivacaine produced continuous analgesia of more than 9 hours in a model of incision pain, approximately 3 times longer than a single free levobupivacaine injection (3 hours). The external ultrasound irradiation can trigger the release of levobupivacaine repeatedly, resulting in on-demand analgesia. In addition, DMSN-bupi-PFP nanoplatforms for ultrasound-enabled analgesia showed low neurotoxicity and good biocompatibility in vitro and in vivo.

Conclusion: This DMSN-bupi-PFP nanoplatform can be used in pain management by providing long-lasting and on-demand pain alleviation with the help of moderate-intensity ultrasound.

Keywords: moderate-intensity ultrasound, phase-transitional, analgesia, nanomedicine

Introduction

Intense postoperative pain is regularly trailed by determined torment in 10–50% of the people.[1–3] Persistent postoperative pain would correlate with delayed hospital discharge and reduce the quality of patients' life.[4–6] Therefore, the management and prevention of persistent postsurgical pain are essential for patient-centric care. Although various anesthetic drugs (such as local anesthetics, cyclooxygenase inhibitors, and opioids) can control pain during and soon after surgery, opioids remain the mainstay of postoperative therapy, even in very localized pain.[7–9] Opioids, on the other hand, have a long list of adverse side effects, including nausea, pruritus, constipation, addiction, tolerance, diversion, and even deadly overdose.[10] Although local anesthetics are commonly used to relieve postoperative pain, their duration of action is limited, and they can have serious cardiovascular or neurological side effects.[11] Furthermore, the intensity of analgesia cannot be adjusted to meet the patient's needs. Although the continuous infusion of local anesthetics through a catheter can provide long-term analgesia, it is not recommended for anticoagulant individuals.[12] Thus, it is essential to develop a robust alternative with superior analgesia performance to manage postoperative pain.[13]

Researchers have focused on manufacturing stimuli-triggerable formulations with ultrasound and near-infrared (NIR) light.[14–16] Compared to NIR-triggered on-demand analgesia-releasing systems, ultrasound was considered an ideal

stimulus due to its advantages in tissue-penetrating depth.[17] Moreover, ultrasonic devices have been commonly used in various clinical settings.[18] However, the stimuli-responsive systems often need higher ultrasonic intensity, which can cause additional burns.[19] Comparatively, microbubbles might provide an ideal choice for constructing new formulations to achieve efficient and safe pain management, but it has been rarely reported so far.[20]

Ultrasonic microbubbles have been widely used in the clinical and provided a physical method to enhance drug delivery in different body parts.[21] Recent clinical trials have demonstrated the safety of microbubbles and provided evidence of the efficacy in the delivery of anticancer agents with ultrasound.[22] The mechanism of improved drug delivery is primarily attributed to the inert cavitation effect and the increase in the interstitial fluid flow.[23] However, under physiological settings, these microbubbles are unstable, and the short half-life of a single injection prevents a long-term analgesic impact. In contrast to traditional ultrasonic microbubbles, perfluoropentane (PFP) is a "liquid-to-gas" phase transition material that is stable in vivo.[23,24] Ultrasound irradiation could initiate the phase transition and convert liquid-phase PFP into gas-phase to enhance the drug delivery process. While most studies have used microbubbles to assist diseases treatment, it is still unclear how to combine these technologies in effective pain management.[24] Moreover, there is a lack of evidence for selective local anesthetics with minimal side effects. The relationship among ultrasonic intensity, postoperative pain relief duration, and biosafety in vivo is yet to be established.

Therefore, for the first time, we introduce dendritic mesoporous silica nanoparticles (DMSN), to investigate their on-demand release performance of ultrasound-triggered local anesthetics. Levobupivacaine, a therapeutically efficacious painkiller with minimal systemic toxicity and limited effects on motor function, was loaded into DMSN. Moreover, PFP was also loaded into the mesoporous channel structure to manufacture ingredient nanoparticles (DMSN-bupi-PFP nanoparticles), giving them ultrasound-sensitive release capabilities with moderate-intensity ultrasound. The PFP acts as a phase-transition unit and achieves fast "liquid-to-gas" transformation under acoustic droplet vaporization (ADV) effect under ultrasound irradiation, which can serve as an ideal material for on-demand local analgesia. Compared to levobupivacaine-loaded DMSN (DMSN-bupi) without PFP encapsulation, a more efficient drug release and significantly improved analgesia effect were observed under moderate ultrasound power density.

Materials and Methods
The Synthesis of Dendritic Mesoporous Silica Nanoparticles
The fabrication of DMSN was obtained, followed by the previously reported method.[25] Two grams of cetyltrimethy-lammonium chloride (CTAC, 25 wt%, Sigma-Aldrich) and triethanolamine (TEA, Sigma-Aldrich) were dissolved in 20 mL water at 95 °C while stirring. After 20 minutes, dropwise additions of the solution involving 1 g tetraethyl orthosilicate (TEOS) and 1.3 g bis[3-(triethoxysilyl)propyl]tetrasulfide (BTES) were made, and the mixture was agitated for another 4 hours. The products were centrifuged and washed numerous times with ethanol and water to eliminate the leftover reactants. The products were extracted twice for 12 hours at 78 °C with a hydrochloric acid (HCl) solution in ethanol (10% v/v) by refluxing to remove the template CTAC.

Characterizations
An FEI Talos F200S electron microscope was used to obtain TEM images, and the corresponding X-ray energy-dispersive spectroscopy (EDS) spectrum was acquired on the same electron microscope performed at 200 kV. The DLS and zeta potential were measured with a Zetasizer Nanoseries (Nano ZS90, Malvern Instrument Ltd) using a distilled water environment at 20°C. ASAP2460 (Micrometrics Instrument Corp) was used to determine the BET surface area and pore-size distribution with N_2 adsorption–desorption technique analysis (Degassing time 6 h, degassing temperature 120°C). A UV-1900i Shimadzu spectroscope with QS-grade quartz cuvettes was used to collect UV-vis-NIR absorption spectra at ambient temperature.

Perfluoropentane and Levobupivacaine Loaded into Dendritic Mesoporous Silica Nanoparticles

DMSN (10 mg) were typically dispersed in the levobupivacaine hydrochloride aqueous solution (2 mg/mL, 5mL) and stirred at room temperature for 12 hours. Then, 200 μL PFP was added and agitated for another 12 hours at room temperature in an ice bath. The suspension was centrifuged for 10 minutes at 12,000 rpm to collect DMSN-bupi-PFP. The supernatant was collected to ascertain the exact loading dose of levobupivacaine. The following equation was used to calculate drug loading efficiency: Drug loading efficiency=1-supernatant amount of levobupivacaine/total levobupivacaine amount.

In vitro Releasing Pattern of Levobupivacaine from Perfluoropentane and Levobupivacaine Dual-Loaded Dendritic Mesoporous Silica Nanoparticles and Levobupivacaine-Loaded Dendritic Mesoporous Silica Nanoparticles

The drug-release profile was conducted based on a previously reported article with modifications.[26] Briefly, DMSN-bupi-PFP and DMSN-bupi at a concentration of 5 mg mL^{-1} were wrapped into dialysis bags (cutoff 3500 Da, Yuanye Biotechnology Co., Ltd, China) and immersed in PBS solution (20 mL) with stirring rate at 160 rpm for 12 h to investigate levobupivacaine release with a constant temperature shaker (MIULAB Co., Ltd, China) in vitro. In the study, the ultrasonic irradiation intensity was 0.6 W cm^{-2} (Dimip Co., Ltd, China). The group with no ultrasound irradiation employed as a control. All tubes were shaken and incubated at 37°C. At specific time intervals, a sample of the release medium (2 mL) was collected for UV-vis inspection to determine the quantity of levobupivacaine released. The tubes (Biofil Co., Ltd, China) were treated with ultrasound (0.6 W cm^{-2}, 1 MHz, 15 min) for 6 times using ultrasonic coupling agents during the time selected for the ultrasound-triggered drug-release experiment. Then, the cumulative release amount of levobupivacaine was calculated based on the corresponding absorbance of the UV-spectrum according to the standard calibration.

Cytotoxicity Evaluation

The standard CCK-8 method was performed to assess the cytotoxicity of DMSN-bupi-PFP. In a 96-well plate, the grown HUVEC cells were seeded and incubated at 37 °C in 5% CO_2. The HUVEC cells were purchased from Sciencell. In the ECM culture medium, DMSN-bupi-PFP at different concentrations (0, 100, 200, 300, 400, and 500 μg mL^{-1}) were added. The medium of HUVEC cells was then removed, and the medium containing varying amounts of DMSN-bupi-PFP was introduced at its location. The media was replaced with the CCK-8 assay (Dojindo, Japan, 100 μL, 10%) after another 12 or 24 hours of incubation, and the cells were incubated for another 2 hours to allow CCK-8 examination. Finally, a microplate reader (Varioskan LUX, Thermo Scientific Inc., USA) was used to measure the viability of HUVEC cells at 450 nm. To assess the safety of ultrasound treatment, the DMSN-bupi-PFP at different concentrations (0, 100, 200, 300, 400, and 500 μg mL^{-1}) was added and incubated with HUVEC cells for 4 h to allow cell internalization. After that, the cells were washed with PBS three times to remove the free DMSN-bupi-PFP in plates. The cells were then exposed to ultrasound irradiation (0.6 W cm^{-2}, 1 MHz, 2 min, duty cycle 50%). The medium was replaced and incubated with the standard CCK-8 assay (Dojindo, Japan, 100 μL, 10%), and a microplate reader was used to determine the viability of HUVEC cells.

Animals

Adult male Balb/c mice (6–8 weeks, 20–25 g), purchased from Liaoning Changsheng Biotechnology Corporation, were used in this study. The studies and methods were carried out in accordance with Dalian Medical University's Institutional Animal Care Committee's requirements. The mice were kept in the 12/12 h light/dark cycle and temperature-controlled environment with sufficient food and drink. Before behavioral testing and surgery, the animals were acclimatized to the nutritional environment for 2 weeks.

Procedures for Establishing the Incision Pain Model in Mice

Using the protocols outlined in the initial study, a mouse model of incision pain was created.[27] For a few minutes, the mice were sedated with 2% isoflurane. A longitudinal incision (2 mm) was made from the proximal border of the heel after

cleaning the left plantar region with a 10% povidone-iodine solution. The bottom muscle is elevated and longitudinally sliced, and then we apply antibiotic ointment after suturing the skin using a 4–0 nylon thread in the center of the incision.

In vivo Drug Administration and Ultrasound Irradiation

It was softly withdrawn after conducting blunt dissection to disclose the sciatic nerve. The incision was sutured with 4–0 nylon and then coated with antibiotic ointment. DMSN-PFP suspension, DMSN-bupi-PFP suspension, DMSN-bupi suspension, PBS solution, or levobupivacaine solution (100 μL, 0.05 mg levobupivacaine per mouse, 5 per group) were injected into the mice around the incision site. The mice were fixed and the hind leg exposed for ultrasonic triggering. Then a gel-coated ultrasonic probe was delivered directly to the injected location using a mild ultrasonic intensity (0.6 W cm^{-2}, 1 MHz, 2 min, duty cycle 50%), which is lower than previously reported.[19,28,29]

Measurement of in vivo Mechanical Allodynia

To measure the response to non-noxious mechanical stimuli in mice, an in vivo mechanical allodynia test was performed using a plantar aesthesiometer (KW-CT, Kaerwen Inc., China). The mice were acclimatized to the test set for 30 min in a plastic cage with a silk mesh floor. Subsequently, the probe was pressed on the sole of the mouse's hind paw, and the force was gradually raised until the mouse retracted its left paw. Hind paws were tested three times, and the paw mechanical threshold (PWT) was automatically adopted. The average was used to determine the PWT (g).

In vivo Thermodynamic Hyperalgesia Measurement

Using the Hargreaves device, thermal Hyperalgesia was determined (KW-LB, Kaerwen Inc., China). On the equipment, the mice were placed on a heating base at 55°C. When the left hind paw was withdrawn, the paw withdrawal latency (PWL) was displayed on the screen. The average of three measurements was calculated for each hind paw. The experiments were conducted at a 5–10 min interval to safeguard the animals, using a 20-second cutoff time.

H&E-Staining and Immunohistochemistry Analysis

At 3 days and 28 days following injection, mice that received DMSN-bupi-PFP with ultrasonic irradiation (0.6 W cm^{-2}, 1 MHz, 2 min) were euthanized. The tissue surrounding the sciatic nerve was removed and preserved overnight in 4% paraformaldehyde. The samples were then dehydrated in graded ethanol and embedded in paraffin for H&E staining. The heart, liver, spleen, lungs, and kidneys were among the major organs removed for H&E staining. Optical microscopy was used to analyze the H&E-stained slices at the injection locations. The mice were heavily sedated for immunohistochemistry examination, and the thoracic cavity was perfused with saline and 4% paraformaldehyde through the left ventricle. After 5 hours, L5 DRG was harvested on the ipsilateral side after PBS, levobupivacaine + US or DMSN-bupi-PFP + US injection. The tissue was simply precooled for 6 hours before being kept in sucrose solution (30%) overnight. After that, the samples were embedded in paraffin and sliced at 3 μm for immunofluorescence staining. A fluorescence microscope (Nikon, TS2) was used to observe and photograph the stained sections.

Statistical Analysis

The statistical analysis was carried out with GraphPad Prism 9 software. A one-way ANOVA was used to examine differences in behavioral evaluations across three treatment groups over different time intervals. The Student's *t*-test was used to compare imaging signals between two groups. The data is provided as a mean value ± standard deviation, and $p < 0.05$ was significant.

Results and Discussion

Design, Synthesis, and Characterization of Perfluoropentane and Levobupivacaine Dual-Loaded Dendritic Mesoporous Silica Nanoparticles

The DMSN was chosen as the carrier for the delivery of levobupivacaine and PFP.[25,30,31] The hollow interior structure of DMSN endows these nanocarriers with high loading capacity. The carrying PFP could achieve a fast "liquid-to-gas" transformation under biomedical ultrasound irradiation, and the levobupivacaine could induce local anesthetics without

apparent side effects.[32] Figure 1A shows the structure of DMSN as seen using transmission electron microscopy (TEM). After the loading of levobupivacaine and PFP, we observe changes in microstructure and morphology in the TEM image (Figure 1B). Zeta potential results showed that the effective loading of levobupivacaine and PFP moderately decreased the absolute value of DMSN (Figure 1C). The diameter of DMSN, DMSN-PFP, and DMSN-bupi-PFP was then measured by dynamic light scattering (DLS). The average hydrodynamic diameters of DMSN, DMSN-PFP, and DMSN-bupi-PFP were found to be 372.0 nm, 379.2 nm, and 485.0 nm, respectively, indicating the success loading of PFP and levobupivacaine (Figure 1D). The N_2 adsorption–desorption technique analysis of DMSN and DMSN-bupi-PFP was used to confirm whether levobupivacaine and PFP could be efficiently loaded into DMSN. DMSN and DMSN-bupi-PFP's surface areas were determined to be 750.3 m^{-2} g^{-1} and 442.1 m^{-2} g^{-1}, with pore volumes of 12.1 nm and 8.8 nm (Figure 1E and F). Therefore, the N_2 adsorption–desorption result confirmed the efficient integration of levobupivacaine and PFP into the
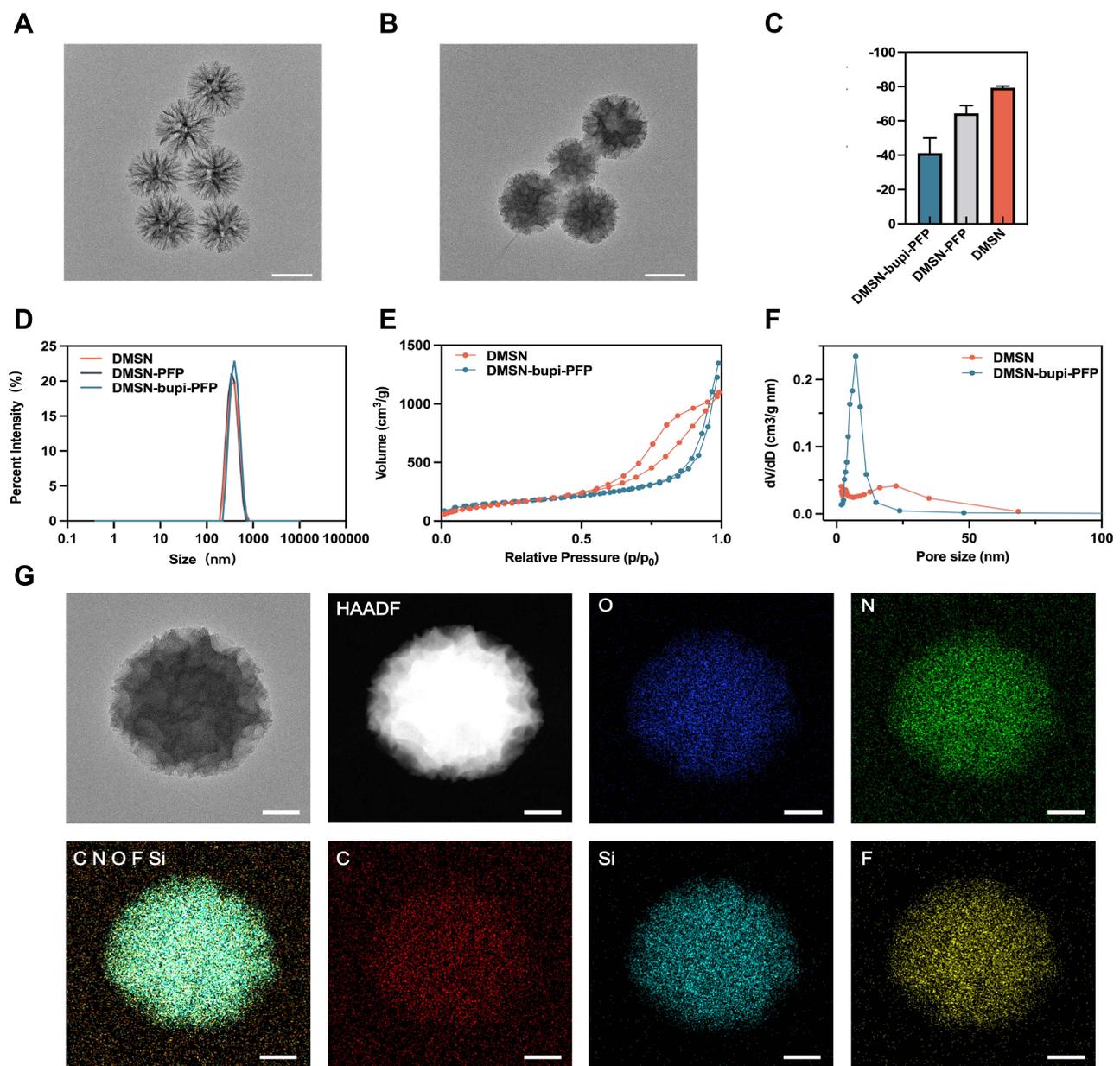

Figure 1 (**A**) TEM image of DMSN. The scale bar is 200 nm. (**B**) TEM image of DMSN-bupi-PFP. The scale bar is 200 nm. (**C**) Zeta potential of DMSN, DMSN-PFP, and DMSN-bupi-PFP. (**D**) Size distribution of DMSN, DMSN-PFP, and DMSN-bupi-PFP. (**E**) N_2 absorption isotherms derived from the BJH pore size distribution curve (**F**) the absorption branch of DMSN and DMSN-bupi-PFP. (**G**) Elemental mapping images derived from DMSN-bupi-PFP. The scale bars are 50 nm.

mesopores. Elemental mapping study showed the presence of C, O, N, Si, and F in DMSN-bupi-PFP, which further revealed the loading of PFP and levobupivacaine into DMSN (Figure 1G). The essential characteristics of DMSN-bupi-PFP were shown as Table S1.

In vitro Ultrasound-Responsive Levobupivacaine Release

To explore the drug-releasing performance of DMSN-bupi-PFP, the UV-Vis spectroscopy of levobupivacaine was acquired. The result showed that the characteristic absorption peak was 263 nm (Figure S1). Moreover, the relationship between the UV absorbance and levobupivacaine concentration was calculated, and the loading efficiency was 91% (Figures S2 and S3). Subsequently, levobupivacaine was measured to investigate the drug-release characteristics of DMSN-bupi-PFP and DMSN-bupi based on UV-Vis absorbance. The release behavior of levobupivacaine triggered by ultrasound was then tested in DMSN-bupi-PFP and DMSN-bupi, respectively. Under ultrasound irradiation, the liquid-to-gas phase change behavior of PFP in the DMSN-bupi-PFP may form gas environment, which could facilitate the formation of ultrasonic cavitation effect and the release of levobupivacaine from the nanoparticles. As shown in Figure 2A, both DMSN-bupi-PFP and DMSN-bupi showed ultrasonic responsive release of levobupivacaine, and the ultrasound response performance followed the order of DMSN-bupi-PFP > DMSN-bupi. The cavitation impact of ultrasound in the presence of PFP, which could break the connection between levobupivacaine molecules and DMSN, is responsible for this unique ultrasound-triggered drug release. The DMSN-bupi-PFP group released more levobupivacaine than the DMSN-bupi group during the six triggering cycles, indicating that DMSN-based nanocarriers have good ultrasonic response adjustable performance. Compared with DMSN-bupi, DMSN-bupi-PFP has more robust ultrasonic responsiveness under the vaporization effect of the acoustic droplet, leading to robust ultrasound-controlled drug-release properties. Therefore, DMSN-bupi-PFP was more sensitive to ultrasound irradiation than DMSN-bupi. In comparison, DMSN-bupi-PFP released a minimal amount of levobupivacaine in 24 hours without ultrasound irradiation, which suggesting that this on-demand drug-delivery nanoplatform is highly controllable in the presence of mild ultrasonic excitation (0.6 W cm^{-2}, 1 MHz, 2 min, duty cycle 50%). The ultrasound intensity in our work is much lower than previously reported articles, which guarantees good safety for biomedical applications.[28,29,33]

Cytotoxicity of Perfluoropentane and Levobupivacaine Dual-Loaded Dendritic Mesoporous Silica Nanoparticles

The cytotoxicity of DMSN-bupi-PFP on human umbilical vein endothelial cells (HUVEC) was evaluated using the standard CCK-8 assay. HUVEC cells, as classical normal cells, are suitable for the evaluation of cytotoxicity of nanomedicine. After coincubation of DMSN-bupi-PFP with HUVEC cells for 24 h, DMSN-bupi-PFP showed good compatibility with HUVEC cells at a high concentration of up to 0.5 mg mL^{-1}, similar to the concentration used in vivo
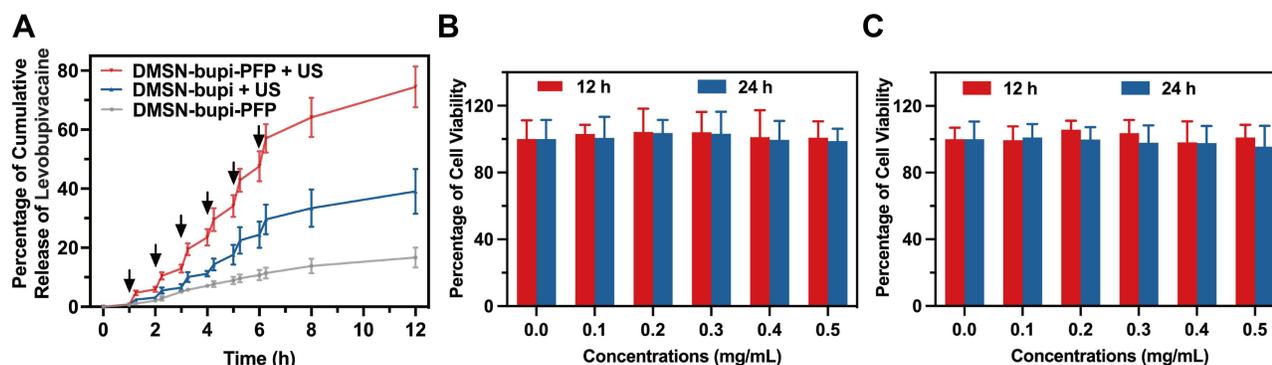

Figure 2 (**A**) Levobupivacaine release performance of DMSN-bupi-PFP and DMSN-bupi under different treatments. (**B**) Cell viability of HUVEC cells treated with varying concentrations of DMSN-bupi-PFP. (**C**) Cell viability of HUVEC cells treated with different concentrations of DMSN-bupi-PFP under ultrasound treatment (0.6 W cm^{-2}, 1 MHz, 50% duty cycle) (n means no difference between groups).

(Figure 2B). Even after ultrasound irradiation for 2 min, negligible cytotoxicity was detected (Figure 2C), indicating the ultrasound-initiated drug-release process with mild-intensity ultrasound irradiation is highly biocompatible.

Ultrasound-Triggered Phase-Transition Behavior in vitro

The PFP-loaded DMSN-bupi-PFP could play an essential role in drug-release efficiency. The ultrasonic imaging test was performed to observe whether DMSN-bupi-PFP could increase the cavitation effect in vitro. DMSN-bupi-PFP, which is known to be easily triggered by ultrasound irradiation in the presence of PFP, produced a much larger microbubble after 5 min of ultrasound irradiation (Figure 3A). Moreover, the vaporization process was confirmed using a medical ultrasound device. When vaporization occurred, a strong signal in both B-mode and contrast-enhanced ultrasound (CEUS)-mode was observed (Figure 3B and C). The DMSN-bupi-PFP NPs, on the other hand, did not produce B-mode and CEUS signals in the irradiated locations. There was no difference between B-mode and CEUS imaging in the non-PFP loading group after irradiation (Figure S4). In contrast, the contrast intensity of B-mode and CEUS images in the PFP group was enhanced more than 100 times. The size of microbubbles was measured to be 953.7 nm after irradiation for 5 minutes (Figure 3D), which is much bigger than DMSN-bupi-PFP without ultrasound irradiation. These mentioned increases are due to the microbubbles generated after 5 minutes of ultrasound irradiation. These findings could support the use of these nanoparticles in cavitation-enhanced drug release with moderate ultrasound irradiation.

In vivo Pain Blockage Triggered by Ultrasound

The mechanical/thermal pain was assessed 3 hours after surgery using the incision pain model.[27] The mechanical and thermal pain were then measured every other hour after injecting different agents or free levobupivacaine. Mechanical hyperalgesia was evaluated via behavioral testing using electronic devices, which could impose mechanical stimulation with a pinpoint, and a corresponding pressure value could be displayed to record the mechanical threshold (Figure 4A-C).[34,35] Moreover, the thermal hyperalgesia was evaluated via behavioral testing, which would generate thermal stimulation at a specific temperature, and the paw-withdrawing time was recorded (Figure 4D-F).[36–38]

Then, in the incision site around the sciatic nerve, levobupivacaine (100 μL, 0.05 mg levobupivacaine per mouse) and DMSN-bupi (100 μL, equal 0.05 mg levobupivacaine per mouse) were administered. Following the injection, ultrasound
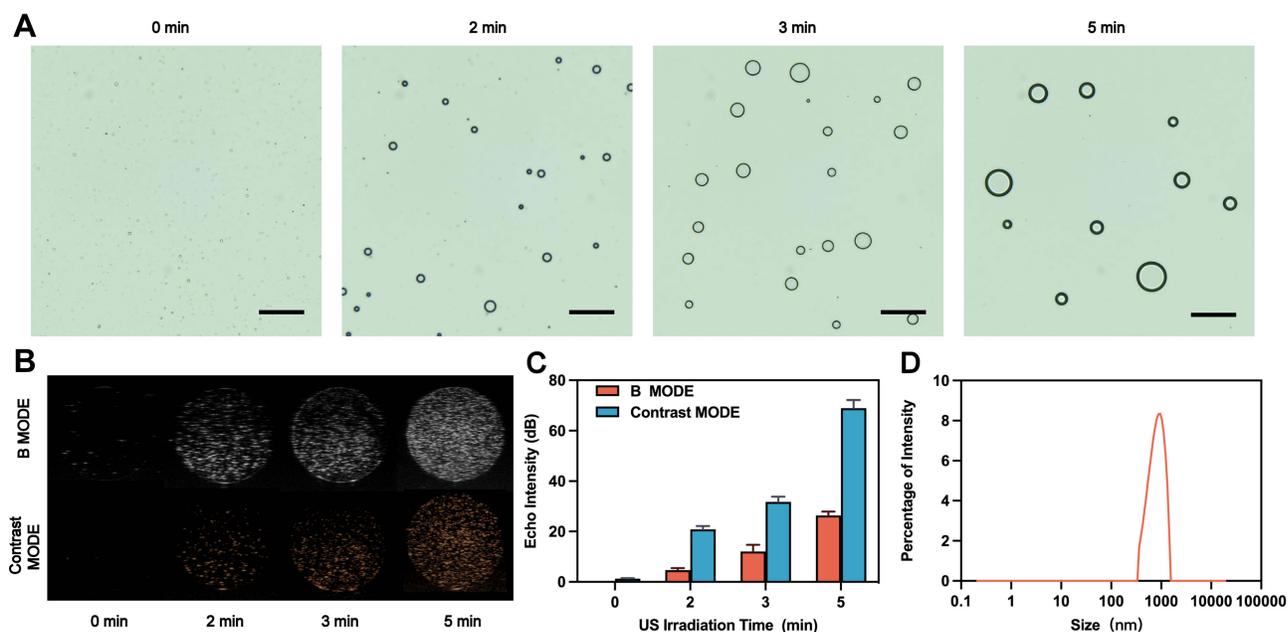

Figure 3 (**A**) Light-microscopy images of the ultrasound-responsive DMSN-bupi-PFP at different time points. Scale bar: 50 μm. (**B**) Ultrasonic image of DMSN-bupi-PFP NPs on B-mode and CEUS-mode imaging at different time points under ultrasound irradiation and (**C**) corresponding quantitative echo intensity (***p < 0.001 among different times compared to 0 min by one-way ANOVA, n=5). (**D**) Size distribution of DMSN-bupi-PFP after ultrasound irradiation for 5 min.
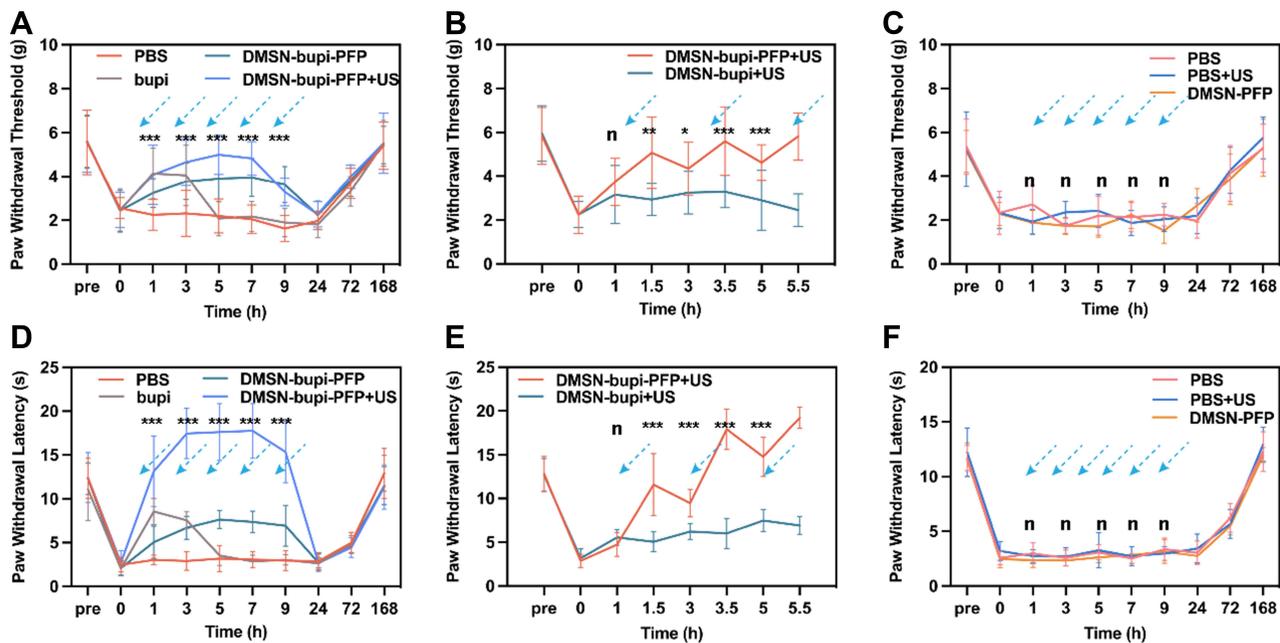
Figure 4 (**A**) Mechanical threshold of mice before and after different treatments in vivo (***$p < 0.001$ between DMSN-bupi-PFP+US and PBS, compared by one-way ANOVA, n=5). (**B**) Mechanical threshold of mice treated by DMSN-bupi-PFP + US and DMSN-bupi + US (n means $p > 0.05$, *$p < 0.05$, **$p < 0.01$, ***$p < 0.001$ between DMSN-bupi-PFP+US and DMSN-bupi+US, compared by t test, n=5). (**C**) Mechanical threshold of mice treated by PBS, PBS+US and DMSN-PFP (n means $p > 0.05$ between groups). (**D**) Thermal latency of mice before and after different treatments (***$p < 0.001$ between ropivacaine and PBS, compared by one-way ANOVA). (**E**) Thermal latency of mice treated by DMSN-bupi-PFP + US and DMSN-bupi + US (n means $p > 0.05$, ***$p < 0.001$ between DMSN-bupi-PFP+US and DMSN-bupi+US, compared by t test, n=5). (**F**) Thermal latency of mice treated by PBS, PBS+US and DMSN-PFP. The blue dotted arrows represent ultrasonic irradiation (0.6 W cm^{-2}, 1 MHz, 2 min) (n means $p > 0.05$ between groups).

treatment was administered immediately, and behavioral assessments were performed 0.5 hours later. The pain threshold measurement result showed that the incision pain model was established successfully 3 h after surgery because the mechanical threshold and thermal latency decreased (Figure 4A). These mice were randomly assigned to different groups. A group of mice receiving sciatic nerve injections of free levobupivacaine showed a burst and transient pain relief. The mechanical threshold and thermal latency increased at 3 h and gradually converged with the PBS group.

The group of mice that received DMSN-bupi-PFP injections in the sciatic nerve had a substantially longer pain control duration, up to 9 hours, indicating that levobupivacaine-loaded nanoparticles may relieve pain for a long time. However, such nanoparticles still cannot respond to changes according to patients' conditions or needs, which is essential for clinical applications. Therefore, the on-demand pain management of DMSN-bupi-PFP with ultrasound as the external stimuli was tested. Group of mice receiving sciatic nerve injections of DMSN-bupi-PFP + US showed more vigorous pain control intensity without reducing the actuation duration, which indicated that ultrasound irradiation has the opportunity to improve pain management. To investigate the role of ultrasound in achieving on-demand pain management, the group that received DMSN-bupi-PFP was treated with ultrasound. In contrast, the group that received DMSN-bupi without the PFP encapsulation was set as a control group (Figure 4B). After ultrasound irradiation for 2 min, a much stronger pain control intensity was achieved in the DMSN-bupi-PFP + US group than the DMSN-bupi + US group, which indicated that the ultrasound responsive properties are essential for the on-demand pain management. The enhanced pain management can be attributed to the burst drug-releasing pattern assisted by the acoustic droplet vaporization effect after acoustic droplet evaporation. Control groups received PBS with ultrasonic irradiation (0.6 W cm^2, 1 MHz, 2 min, duty cycle 50%) and DMSN-PFP injection alone to eliminate the influence of ultrasound and DMSN-PFP (Figure 4C). The PBS group, PBS+US group, and the DMSN-PFP group all had no meaningful effect on pain reduction, suggesting that the DMSN-bupi-PFP with ultrasonic response inhibited incision pain.

Similarly, mice receiving sciatic nerve injection of DMSN-bupi-PFP increased the thermal latency on 55 °C hot plates compared to that of free levobupivacaine, indicating that DMSN-bupi-PFP could prolong pain management (Figure 4D).

The thermal latency lasted for only 3 h and gradually converged with the PBS group. Mice injected with DMSN-bupi-PFP + US showed improved thermal latency capability, suggesting that ultrasound irradiation has the opportunity to improve pain management by the acoustic droplet vaporization effect. The PFP encapsulation could induce a gas environment to support more robust levobupivacaine release (Figure 4E). As controls, no significant analgesic effect was detected among PBS group, PBS + US group, and DMSN-PFP + US, which further proved that ultrasound responsive DMSN-bupi-PFP + US could block incision pain (Figure 4F). After 168 hours, all groups' mechanical thresholds and thermal latency recovered to baseline, demonstrating the incision pain model is a standard operation.

L5 Dorsal Root Ganglion Immunofluorescence Analysis

Since tissue injury can cause a decreased nociceptive threshold by increasing the responsiveness of peripheral afferent neurons, the incision pain block was evaluated with immunofluorescence analysis. The L5 Dorsal Root Ganglion (DRG) on the ipsilateral side was extracted for immunofluorescence testing because the L4 and L5 DRG axons make up the majority of the axons in the sciatic nerve. c-fos is a rapidly activated early gene that can indicate a cell's activation state.[39,40] TRPV1 is a nonselective cation channel that plays a role in several types of hyperalgesia caused by tissue injury.[41,42] Therefore, double-labeling neurons with TRPV1 and c-fos is selected for pain-related behavioral assessments. After treating with different agents for 5 h, immunofluorescence staining result of L5 DRG revealed that the number of neurons doubly labeled for c-fos and TRPV1 was significantly reduced in both the DMSN-bupi-PFP + US and DMSN-bupi + US groups as compared to the levobupivacaine + US group (Figure 5). The reduced expression of c-fos and TRPV1 indicated that the levobupivacaine released by DMSN persisted and the postoperative pain was successfully blocked. Moreover, DMSN-bupi-PFP showed much lower expression of c-fos and TRPV1 after three repeated ultrasonic triggering cycles than DMSN-bupi, indicating that DMSN-bupi-PFP was more ultrasonically controllable. Thus, ultrasound irradiation assisted stable incision pain block successfully relieved levobupivacaine-related pain in an on-demand manner.

Neurotoxicity and Histocompatibility Assays in vitro and in vivo

Mice that received injections of DMSN-bupi-PFP combined with ultrasonic irradiation were euthanized on 3 days and 28 days after injection to highlight the potential histocompatibility of DMSN-bupi-PFP in pain management.[43] The sciatic nerve and surrounding muscle tissues were harvested and sectioned for histological analysis. Representative tissue reaction to DMSN-bupi-PFP was evaluated with hematoxylin–eosin (H&E) staining and toluidine blue staining. The tissues were neither edematous nor discolored, and there were no other apparent indicators of tissue damage (Figure 6A and B). The toluidine blue-stained slices of the sciatic nerves in rats injected
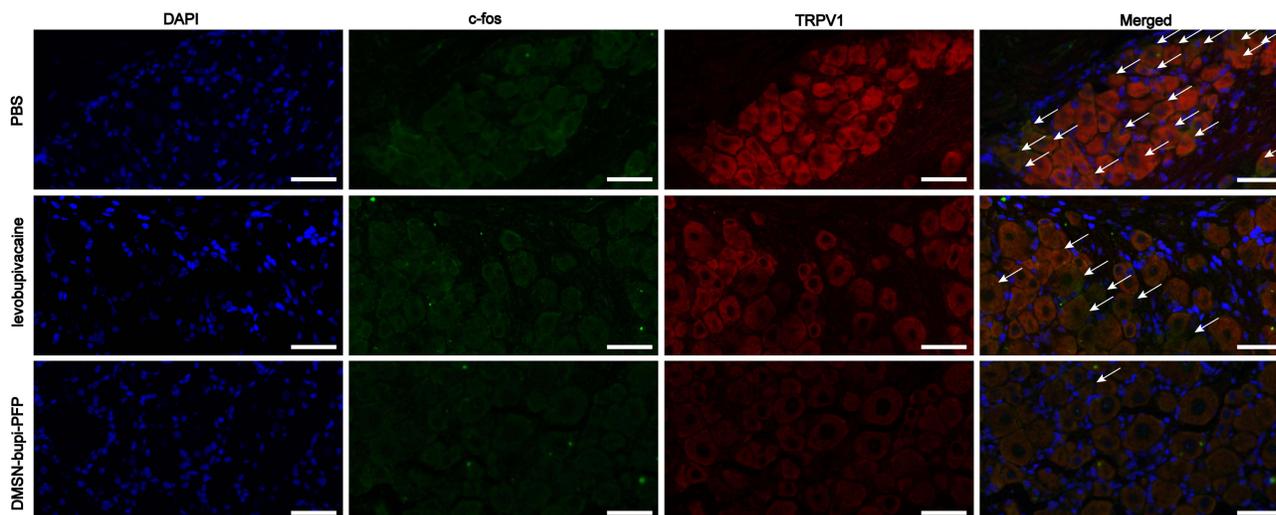

Figure 5 DAPI, c-fos, and TRPV1 co-staining immunofluorescence results of L5 DRG after different treatments followed by ultrasound irradiation. The scale bars are 50 μm.
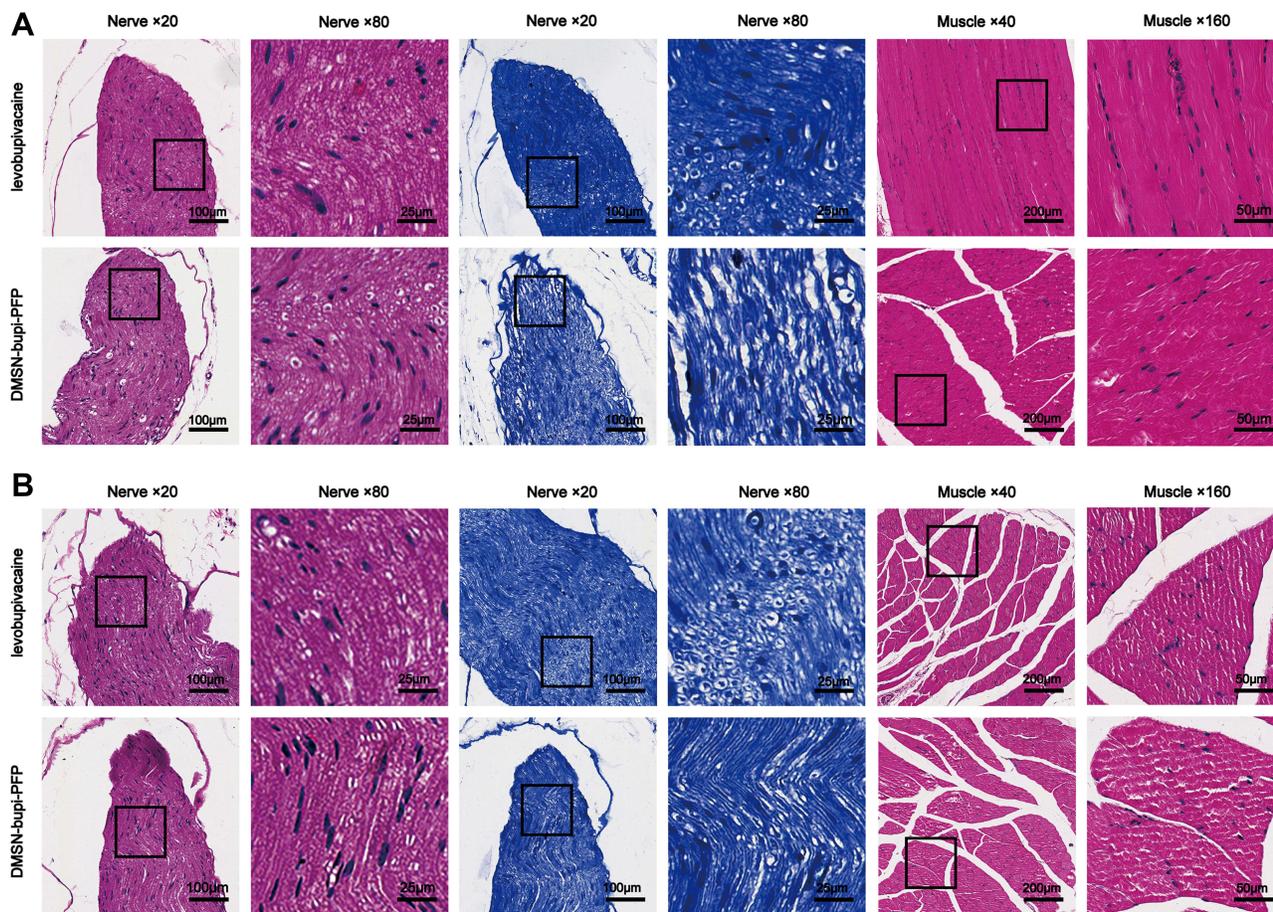
Figure 6 H&E staining and toluidine blue staining results from the sciatic nerve and surrounding muscle at (**A**) 3 days and (**B**) 28 days. The scale bars are 100 μm.

with DMSN-bupi-PFP were obtained due to the low diagnostic resolution of H&E staining for nerve injury. The Nessoids of nerve cells can be stained with toluidine blue staining solution, which is the crucial indicator of nerve cell injury.[44] At 3 days and 28 days following ultrasonic irradiation, minimal peripheral damage with decreased axon density was identified. As a result, these findings showed that DMSN-bupi-PFP nanoplatforms paired with in vivo ultrasonic irradiation for on-demand pain treatment have high biocompatibility.

In addition to the efficacy of on-demand pain therapy, the biocompatibility of levebupivacaine and DMSN-bupi-PFP was investigated in vivo. H&E staining figures of major organs (such as the heart, liver, spleen, lungs, and kidneys) from mice treated with levobupivacaine and DMSN-bupi-PFP revealed no significant abnormalities or distinct tissue damage (Figure 7), indicating that levobupivacaine and DMSN-bupi-PFP have negligible toxicity to the major organs.
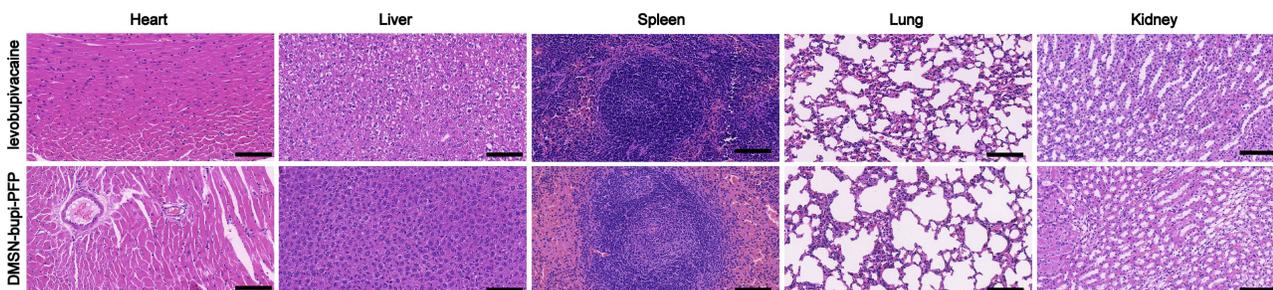

Figure 7 H&E staining results of the major organs (including heart, liver, spleen, lungs, and kidneys). The scale bars are 100 μm.

Discussion

The invention of a nanoplatform that generated on-demand persistent analgesia is described in this work. Our findings in the incision pain model in mice suggest that the DMSN-bupi-PFP may improve ultrasonic responsive sensitivity to release levebupivacaine. The method potentially might provide an advantage over currently used analgesia to manage postoperative pain in that their drug-release performance can be almost enhanced simply by ultrasound-triggered liquid-to-gas phenomenon. In addition, these nanoplatforms can extend the duration of analgesia generated by triggering the drug-release mechanism.

Although several studies have demonstrated the light-triggered on-demand pain management, the application was restricted by penetration depth of light. For example, Zhang et al developed a macromolecular prodrug in which a photo-cleavable coumarin linkage connects the local anesthetic tetracaine to the polymer poloxamer 407.[45] The macromolecular prodrug has no anesthetic action without light irradiation, while treated with a low-power blue light-emitting diode can result in local anesthesia. The low-penetration light made it difficult for clinical applications.

Ultrasound was deemed an excellent stimulus over NIR-triggered on-demand analgesia-releasing systems because of its superior tissue-penetrating depth. Rwei have constructed ultrasound-triggered administration of an anesthetic from liposomes to improve the depth of stimuli-responsive systems.[46] They demonstrate in vivo reproducible ultrasound-triggered nerve blocks, with nerve-block length varying depending on the extent and intensity of ultrasound. However, the stimuli-responsive systems often require higher ultrasonic intensity, which can result in more burns in vivo. At different times following ultrasonic irradiation, minimal peripheral nerve and the major organs damage were identified in our study, indicating that DMSN-bupi-PFP and our applicable strategy have negligible toxicity to the major organs.

The hypothesis that ultrasound irradiation could initiate a liquid-to-gas transition supported the ultrasound-triggered levebupivacaine release in vitro. PFP is a stable "liquid-to-gas" phase transition material in vivo and ultrasound irradiation could trigger the phase change and convert liquid-phase PFP to a gas phase. Because of the inert cavitation effect and enhanced interstitial fluid flow, microbubbles can be a great candidate for designing new formulations for effective and safe pain management. In the presence of gas-phase PFP, the cavitation impact of ultrasound could disrupt the interaction between levobupivacaine molecules and DMSN to achieve on-demand pain management. Compared to sonodynamic effect-triggered drug release, our study showed that the pain management could be adjusted with moderate-intensity ultrasound, which is milder than previous articles for clinical applications. No obvious cell or tissue damage was observed in our test model.

Moreover, although local anesthetics are commonly used to relieve postoperative pain, their duration of action is limited. Nanotechnology is a crucial method to prolong the duration of local anesthetics. For example, Berrocoso et al described an oral nanosystem that offered sustained and prolonged analgesia in an animal model of neuropathic pain for more than 7 days.[13] However, the system still lacks stimuli-responsive properties. Using the incision pain model, we demonstrate that DMSN-bupi-PFP could prolong the duration of levobupivacaine to 9 hours with both thermal latency and mechanical hyperalgesia examination. Moreover, the DMSN-bupi-PFP has the opportunity to improve pain management with ultrasound irradiation. The enhanced pain management can be attributed to the burst drug-releasing pattern assisted with the acoustic droplet vaporization effect after acoustic droplet evaporation.

Conclusion

In conclusion, we reported an on-demand nanoplatform that caused persistent analgesia for the first time. The nanoplatform has the potential to overcome the limitations of standard pain treatment and improve local anesthetic pain control. Ultrasound irradiation could initiate the phase-transition process of PFP and convert liquid phase PFP into gas phase to enhance the cavitation effect and reduce ultrasonic intensity. Ultrasound irradiation increased the release of levobupivacaine, which could help postoperative patients with on-demand analgesia and better pain management in incision sites. The reduced ultrasonic intensity guarantees the biosafety of the pain relief process. In addition, the low neurotoxicity and high histocompatibility of these nanoplatforms were validated in vitro and in vivo, indicating their potential for future clinical translation. This study broadened the new application for DMSN as nanocarriers in pain management and offered a long-lasting and on-demand pain-controlling treatment modality based on ultrasonic irradiation.

Acknowledgments

Supplementary Materials

Supplementary figures and tables are available in the Supplemntary Materials file.

Disclosure

The authors report no conflicts of interest in relation to this work.

References

1. The L. Rethinking chronic pain. *Lancet*. 2021;397(10289):2023.
2. Kopf A, Gjoni E. [Multimodal therapy programs for chronic pain]. *Anaesthesist*. 2015;64(2):95–107. Chinese.
3. Treede RD, Rief W, Barke A, et al. Chronic pain as a symptom or a disease: the IASP Classification of Chronic Pain for the International Classification of Diseases (ICD-11). *Pain*. 2019;160(1):19–27.
4. Bushnell MC, Ceko M, Low LA. Cognitive and emotional control of pain and its disruption in chronic pain. *Nat Rev Neurosci*. 2013;14 (7):502–511.
5. Cohen SP, Vase L, Hooten WM. Chronic pain: an update on burden, best practices, and new advances. *Lancet*. 2021;397(10289):2082–2097.
6. Kohrt BA, Griffith JL, Patel V. Chronic pain and mental health: integrated solutions for global problems. *Pain*. 2018;159(Suppl 1):S85–S90.
7. Bruehl S. Complex regional pain syndrome. *BMJ*. 2015;351:h2730.
8. Raymond TJ, Tobin KA, Rogers TS. Nonopioid pharmacologic treatments for chronic pain. *Am Fam Physician*. 2021;103(9):561–565.
9. Kiyatkin EA. Respiratory depression and brain hypoxia induced by opioid drugs: morphine, oxycodone, heroin, and fentanyl. *Neuropharmacology*. 2019;151:219–226.
10. Corder G, Castro DC, Bruchas MR, Scherrer G. Endogenous and exogenous opioids in pain. *Annu Rev Neurosci*. 2018;41:453–473.
11. Yoon E, Babar A, Choudhary M, Kutner M, Pyrsopoulos N. Acetaminophen-induced hepatotoxicity: a comprehensive update. *J Clin Transl Hepatol*. 2016;4(2):131–142.
12. Horlocker TT. Regional anaesthesia in the patient receiving antithrombotic and antiplatelet therapy. *Br J Anaesth*. 2011;107(Suppl 1):i96–106.
13. Berrocoso E, Rey-Brea R, Fernandez-Arevalo M, Mico JA, Martin-Banderas L. Single oral dose of cannabinoid derivate loaded PLGA nanocarriers relieves neuropathic pain for eleven days. *Nanomedicine*. 2017;13(8):2623–2632.
14. Zhan C, Wang W, Santamaria C, et al. Ultrasensitive phototriggered local anesthesia. *Nano Lett*. 2017;17(2):660–665.
15. Qiao B, Luo Y, Cheng HB, et al. Artificial nanotargeted cells with stable photothermal performance for multimodal imaging-guided tumor-specific therapy. *ACS Nano*. 2020;14(10):12652–12667.
16. Cheng HB, Qiao B, Li H, et al. Protein-activatable diarylethene monomer as a smart trigger of noninvasive control over reversible generation of singlet oxygen: a facile, switchable, theranostic strategy for photodynamic-immunotherapy. *J Am Chem Soc*. 2021;143(5):2413–2422.
17. Jiang Q, Qiao B, Lin X, et al. A hydrogen peroxide economizer for on-demand oxygen production-assisted robust sonodynamic immunotherapy. *Theranostics*. 2022;12(1):59–75.
18. Gupta I, Eisenbrey JR, Machado P, et al. Diagnosing portal hypertension with noninvasive subharmonic pressure estimates from a US contrast agent. *Radiology*. 2021;298(1):104–111.
19. Athanassiadis AG, Ma Z, Moreno-Gomez N, et al. Ultrasound-responsive systems as components for smart materials. *Chem Rev*. 2021;1:548.
20. Rabut C, Yoo S, Hurt RC, et al. Ultrasound technologies for imaging and modulating neural activity. *Neuron*. 2020;108(1):93–110.
21. Snipstad S, Vikedal K, Maardalen M, Kurbatskaya A, Sulheim E, Davies CL. Ultrasound and microbubbles to beat barriers in tumors: improving delivery of nanomedicine. *Adv Drug Deliv Rev*. 2021;177:113847.
22. Feltham T, Paudel S, Lobao M, Schon L, Zhang Z. Low-intensity pulsed ultrasound suppresses synovial macrophage infiltration and inflammation in injured knees in rats. *Ultrasound Med Biol*. 2021;47(4):1045–1053.
23. Meng L, Liu X, Wang Y, et al. Sonoporation of cells by a parallel stable cavitation microbubble array. *Adv Sci*. 2019;6(17):1900557.
24. Bhansali D, Teng SL, Lee CS, Schmidt BL, Bunnett NW, Leong KW. Nanotechnology for pain management: current and future therapeutic interventions. *Nano Today*. 2021;2:39.
25. Wu M, Meng Q, Chen Y, et al. Large-pore ultrasmall mesoporous organosilica nanoparticles: micelle/precursor co-templating assembly and nuclear-targeted gene delivery. *Adv Mater*. 2015;27(2):215–222.
26. Luo Y, Qiao B, Zhang P, et al. TME-activatable theranostic nanoplatform with ATP burning capability for tumor sensitization and synergistic therapy. *Theranostics*. 2020;10(15):6987–7001.
27. Pogatzki EM, Raja SN. A mouse model of incisional pain. *Anesthesiology*. 2003;99(4):1023–1027.
28. Li Y, Teng X, Yang C, et al. Ultrasound Controlled Anti-Inflammatory Polarization of Platelet Decorated Microglia for Targeted Ischemic Stroke Therapy. *Angew Chem Int Ed Engl*. 2021;60(10):5083–5090.
29. Meng Z, Zhang Y, She J, et al. Ultrasound-mediated remotely controlled nanovaccine delivery for tumor vaccination and individualized cancer immunotherapy. *Nano Lett*. 2021;21(3):1228–1237.
30. Xu C, Lei C, Wang Y, Yu C. Dendritic mesoporous nanoparticles: structure, synthesis and properties. *Angew Chem Int Ed Engl*. 2022;61(12): e202112752.
31. Gao F, Lei C, Liu Y, et al. Rational design of dendritic mesoporous silica nanoparticles' surface chemistry for quantum dot enrichment and an ultrasensitive lateral flow immunoassay. *ACS Appl Mater Interfaces*. 2021;13(18):21507–21515.

32. Heppolette CAA, Brunnen D, Bampoe S, Odor PM. Clinical pharmacokinetics and pharmacodynamics of levobupivacaine. *Clin Pharmacokinet.* 2020;59(6):715–745.

33. Wang Z, Liu B, Sun Q, et al. Upconverted metal-organic framework janus architecture for near-infrared and ultrasound co-enhanced high performance tumor therapy. *ACS Nano.* 2021.

34. Costa S, Muscara MN, Allain T, et al. Enhanced analgesic effects and gastrointestinal safety of a novel, hydrogen sulfide-releasing anti-inflammatory drug (ATB-352): a role for endogenous cannabinoids. *Antioxid Redox Signal.* 2020;33(14):1003–1009.

35. Kartha S, Yan L, Ita ME, et al. Phospholipase A2 inhibitor-loaded phospholipid micelles abolish neuropathic pain. *ACS Nano.* 2020;14 (7):8103–8115.

36. Moutal A, Cai S, Yu J, et al. Studies on CRMP2 SUMOylation-deficient transgenic mice identify sex-specific Nav1.7 regulation in the pathogenesis of chronic neuropathic pain. *Pain.* 2020;161(11):2629–2651.

37. Corder G, Tawfik VL, Wang D, et al. Loss of mu opioid receptor signaling in nociceptors, but not microglia, abrogates morphine tolerance without disrupting analgesia. *Nat Med.* 2017;23(2):164–173.

38. Pogatzki-Zahn EM, Gomez-Varela D, Erdmann G, Kaschube K, Segelcke D, Schmidt M. A proteome signature for acute incisional pain in dorsal root ganglia of mice. *Pain.* 2021;162(7):2070–2086.

39. Bonapersona V, Schuler H, Damsteegt R, et al. The mouse brain after foot shock in four dimensions: temporal dynamics at a single-cell resolution. *Proc Natl Acad Sci U S A.* 2022;119(8):548.

40. Joo JY, Schaukowitch K, Farbiak L, Kilaru G, Kim TK. Stimulus-specific combinatorial functionality of neuronal c-fos enhancers. *Nat Neurosci.* 2016;19(1):75–83.

41. Lee SH, Tonello R, Im ST, et al. Resolvin D3 controls mouse and human TRPV1-positive neurons and preclinical progression of psoriasis. *Theranostics.* 2020;10(26):12111–12126.

42. Ortiz-Renteria M, Juarez-Contreras R, Gonzalez-Ramirez R, et al. TRPV1 channels and the progesterone receptor Sig-1R interact to regulate pain. *Proc Natl Acad Sci U S A.* 2018;115(7):E1657–E1666.

43. Gao X, Zhu P, Yu L, Yang L, Chen Y. Ultrasound/acidity-triggered and nanoparticle-enabled analgesia. *Adv Healthc Mater.* 2019;8(9):e1801350.

44. Zhao C, Liu A, Santamaria CM, et al. Polymer-tetrodotoxin conjugates to induce prolonged duration local anesthesia with minimal toxicity. *Nat Commun.* 2019;10(1):2566.

45. Zhang W, Ji T, Li Y, et al. Light-triggered release of conventional local anesthetics from a macromolecular prodrug for on-demand local anesthesia. *Nat Commun.* 2020;11(1):2323

46. Rwei AY, Paris JL, Wang B, et al. Ultrasound-triggered local anaesthesia. *Nat Biomed Eng..* 2017;1:644-653